J|A|C|S COMMUNICATIONS

Published on Web 11/23/2010

Kinetic Analysis of the M2 Proton Conduction of the Influenza Virus

Rafal M. Pielak and James J. Chou*

Department of Biological Chemistry and Molecular Pharmacology, Harvard Medical School, Boston, Massachusetts 02115, United States, and Program in Biological and Biomedical Sciences, Harvard Medical School, Boston, Massachusetts 02115, United States

Received September 19, 2010; E-mail: chou@cmcd.hms.harvard.edu

Abstract: The M2 protein of the flu virus forms a proton selective channel that is necessary for viral replication. The channel has a slow rate of conduction but attains near perfect selectivity for protons. Many models have been proposed to explain the mechanism of proton conduction based on whole cell channel recordings and molecular dynamics simulations, but a detailed kinetic analysis of the channel activity has not yet been performed. We obtained detailed conduction vs pH measurements for M2 and a number of its variants using a sensitive and reproducible liposome proton flux assay. The proton transport follows Michaelis−Menten-like kinetics with two saturation steps: one pseudosaturation at pH ∼5.5, and another full saturation at pH ∼4. The heart of the mechanism is the pore-lining His37 and Trp41. NMR measurements suggest that histidine and tryptophan act in unison to transport protons down the concentration gradient. The log of apparent K_m derived from the kinetics data matches closely to the histidine pK_a and correlates with chemical shift perturbation of the Trp41 gate, indicating that histidine protonation and opening of the channel gate are synchronized events. Finally, mutagenesis and structural analysis identified key residues that affect the rate of conduction.

The M2 protein forms a pH-dependent, proton-selective channel in the envelope of the flu A virus.[1] Recent high resolution structures of M2 show that the channel domain is a left-handed four helix bundle with a well-defined hydrophilic pore and that two conserved residues inside the pore, His37 and Trp41, physically occlude the C-terminal end of the pore.[2−4] Early whole cell channel recordings showed that His37 is essential for proton selectivity[5] and that Trp41 may be responsible for unidirectional conductance.[6]

In the closed state, the four Trp41 indoles form a tight hydrophobic ring (∼1.4 Å in diameter) that is too small to allow ions to pass; they are mostly locked. The three-bond scalar coupling constant between backbone ^{15}N and side chain $^{13}C_\gamma$ of Trp41 is 2.6 Hz, indicating that the χ_1 rotamer is locked at the *trans* conformation. Moreover, Trp41 χ_2 is fixed at around −120° according to nuclear Overhauser effects (NOEs) and residual dipolar coupling data.[2] The indoles become unlocked as the channel is activated at lower pH. Relaxation-compensated Carr−Purcell−Meiboom−Gill (CPMG)[7] measurement of μs−ms time scale dynamics of the indole amine showed that as the pH was lowered from 7.5 to 6.0, the chemical exchange rate increased by more than 4-fold.[2] Clearly, the dynamics of Trp41 indoles is coupled to channel activation, either through destabilization of transmembrane (TM) helix−helix packing in the open state or through interaction with protonated His37 imidazoles, or both. The Trp41 indole is frequently called the channel gate.

Since proton conduction is pH-dependent, protonation of His37 imidazoles is important for the mechanism. pH titration by solid-state NMR (ssNMR) revealed three distinct pK_a values of His37: 8.2, 6.3, and one below 5.[8] Both solution and crystal structures show that the histidines are close enough to interact with each other.[2,4] A previous channel recording experiment showed that the rate of conduction is strongly pH-dependent and that the rate saturates at pH ≈ 4.[5,9] These studies however only recorded five[9] or three[5] pH points in the pH range 7−5.5 and thus did not observe other pK_a values reported by the ssNMR measurements.

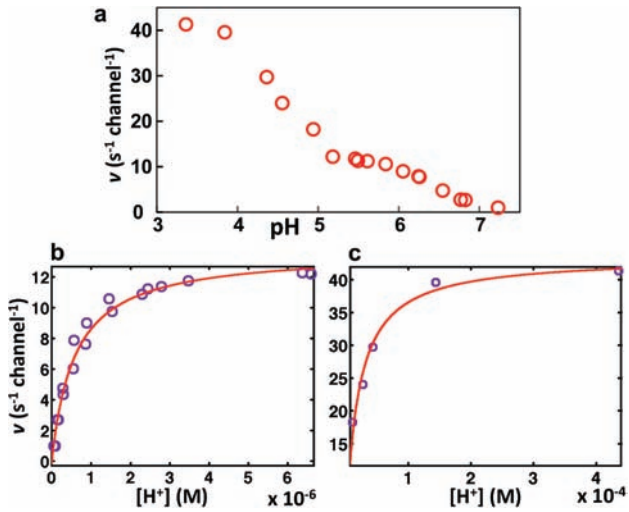

Figure 1. Dependence of the rate of H^+ conduction (υ) on pH for $M2_{18-60}$. (a) υ vs pH in pH range 7.2−3.4, showing multiple inflection points. (b and c) The same data as in (a), but plotted as a function of $[H^+]$ for the pH range 7.2−5.2 and 5.0−3.4, respectively.

Here, we carried out much more detailed measurements of proton conduction vs pH, showing that the proton flux follows Michaelis−Menten-like kinetics with two saturation steps. Functional mutagenesis also identified key residues that affect the rate of conduction. In addition, His37 pK_a and Trp41 chemical shift perturbation were measured by solution NMR for the $M2_{18-60}$ construct. Our results suggest that M2 is a proton transporter, in which histidine and tryptophan act in unison to transport protons down the concentration gradient.

We previously developed a liposome-based assay that closely mimics proton flux from the acidic endosome into the virus after endocytosis of the virus.[3] The same assay was used here to investigate the pH-dependence of M2 proton transport. We measured the initial rates of proton conduction (υ) for various starting pH values from 7.2 to 3.4 or equivalently proton concentration ($[H^+]$) from 6.3×10^{-8} to 4×10^{-4} M (see Figure S1 in the Supporting Information (SI) for examples of raw data). The υ vs pH/$[H^+]$ plot in Figure 1 shows two saturation steps: one pseudosaturation at pH ∼5.5 and one full saturation at pH ∼4. Only the first saturation step is physiologically relevant. The extracellular

pH is ~7.4, and hemagglutinin-mediated membrane fusion occurs at pH ~5.4.[10,11] M2 evolved to function in the pH range 7.4−5.4, and therefore the first saturation step is relevant to understanding the mechanism of proton conduction in the native-like environment. The data in Figure 1 can be fit to a simple saturation-kinetics equation:

$$\upsilon = \frac{\upsilon_{max}[H_N^+]}{K_{app} + [H_N^+]} \quad (1)$$

where $\upsilon_{max} = k_{trans}[M2]_0$ and $[M2]_0$ is the concentration of the active M2 channel. The fit results in a k_{trans} (rate of transport) of 14 H^+ s^{-1} and pK_{app}(−log K_{app}) of 6.25 for the pH range 7.2−5.2 and k_{trans} of 40 H^+ s^{-1} and pK_{app} of 4.7 for the pH range 5.0−3.4. The pK_{app} values are consistent with the three different pK_a's (8.2, 6.3, <5) observed by ssNMR.[8] It was proposed in ref 8 that in the closed state two pairs of histidines in the tetramer each share one proton, which explains the high pK_a ~8.2. This proposal was further supported by recent molecular dynamics simulation.[12] Lowering the pH results in the third protonation event that, in turn, results in disruption of the two histidine dimers and proton conduction. The fourth protonation is shifted to an even lower pH due to the close presence of three positively charged histidines. The close agreement between the pK_{app} values derived from conduction kinetics and the histidine pK_a's suggests that the protonation and the subsequent deprotonation of His37 are important events during the proton transport. This result is consistent with the ssNMR measurement of pH-dependent His37 tautomerization in the lipid bilayer.[13]

Since the Trp41 indoles are mostly locked in the closed state, His37 protonation must result in conformational changes that lead to the opening of the tryptophan gates. To investigate the His37-Trp41 relation, we conducted a pH titration of His37 and measured its effect on the chemical shift of the Trp41 indole amino group. We specifically ^{13}C-labeled the His37 imidazole and measured the $^{13}C_{\varepsilon 1}$ peak of His37 at different pH values by direct ^{13}C observation. At pH 7.3, a strong $^{13}C_{\varepsilon 1}$ resonance corresponding to an unprotonated imidazole was observed at 138 ppm. This peak then reduced in height and increased in line width as the pH decreased. At the same time, two new $^{13}C_{\varepsilon 1}$ peaks gradually appeared at 131 and 123 ppm (Figure 2a). These two peaks probably correspond to the protonated states of the imidazole. The data suggest that, during activation at low pH, there are at least three chemical or conformational states of the His37 imidazole, for instance an unprotonated state and two distinct conformations of the protonated state. These states are in slow exchange, slower than the difference of the carbon chemical shifts evolution at ~1000 per sec. Hz. This slow rate of His37 conformational exchange is consistent with the slow rate of proton conduction.

The pH titration data for the $^{13}C_{\varepsilon 1}$ resonance at 138 ppm were fit to the Hill equation (Supporting Methods in the SI) yielding a pK_a of ~6.6 (Figure 2b). A similar pH titration of the Trp41 indole amino group resulted in a pK_C (−log K(conformational)) of 6.8 (Figure 2c). The close agreement between the pK_a of His37 and the pK_C of Trp41 suggests that protonation/deprotonation of His37 is coupled to the conformational transition of the Trp41 indole. The synchronization between the two events is consistent with earlier flourescence and Raman spectroscopy studies that suggested the presence of cation−π interaction between the two residues upon histidine protonation.[14]

The available structural and functional data suggest that multiple factors could influence the rate of conduction: the rate of proton entrance, the proton relay inside the channel, the His37 protonation, the His37/Trp41 interaction resulting in the gate opening, and the rate of proton exit at the C-terminal end of the channel. We investigated these factors by measuring the pH-dependence of proton flux for three M2 mutants: V27A, S31A, and D44A. All three mutants show the saturation of proton flux in the pH range ~7−5. Fitting the data to eq 1, however, yields substantially different k_{trans} values (Figure 3a; Table S1). V27A is one of the most prominent drug resistant mutants of M2, and its k_{trans} is more than 2-fold higher than that of WT. The structure of V27A[15] (PDB code: 2KWX) is overall very similar to that of WT[2] (PDB code: 2RLF). An obvious difference is that replacing the side chains of Val27 with the smaller alanines resulted in an enlarged N-terminal opening of the channel. In WT, the N-terminal entrance is constricted to ~2.5 Å by the packing of hydrophobic side chains

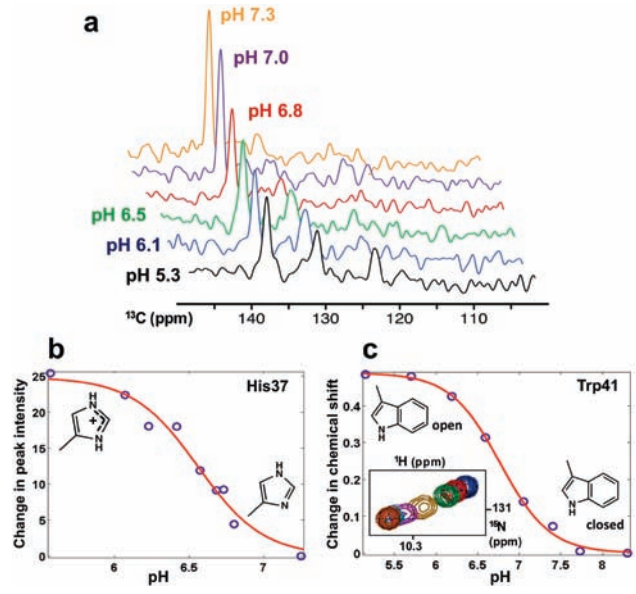

Figure 2. Synchronized conformational changes of His37 and Trp41. (a) A series of 1D carbon spectra from pH 7.3 to 5.0 show the $^{13}C_{\varepsilon 1}$ resonances at 138 ppm, corresponding to unprotonated His37 imidazole. It broadens and decreases in size as pH is lowered. At the same time, two new peaks of $^{13}C_{\varepsilon 1}$ gradually appear at 131 and 123 ppm. The spectra of the double mutant containing only one histidine (His37) are shown here for clarity (see Supporting Methods). (b) The pH titration data of the WT for the $^{13}C_{\varepsilon 1}$ resonance at 138 ppm were fit to the Hill equation, and the fit yielded a pK_a of ~6.6. (c) A similar pH titration of the indole amino proton resonance of Trp41 resulted in a pK_C (−log K(conformational)) of ~6.8.

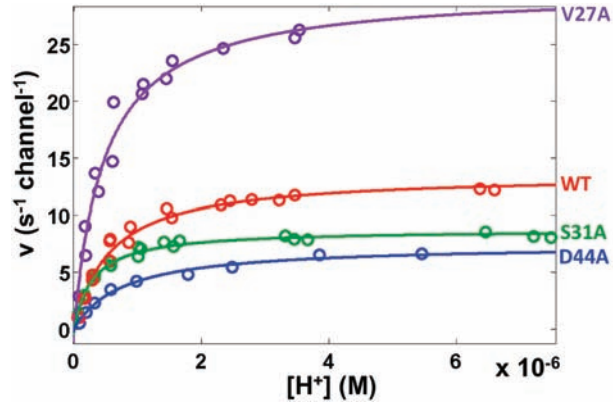

Figure 3. M2 mutants kinetics. The υ vs H^+ concentration curves for WT (k_{trans} ≈ 14.0 H^+ s^{-1}, K_{app} ≈ 5.7 × 10^{-7} M; red), V27A (k_{trans} ≈ 30.1 H^+ s^{-1}, K_{app} ≈ 5.1 × 10^{-7} M; violet), S31A (k_{trans} ≈ 8.6 H^+ s^{-1}, K_{app} ≈ 3.0 × 10^{-7} M; green), and D44A (k_{trans} ≈ 7.5 H^+ s^{-1}, K_{app} ≈ 7.7 × 10^{-7} M; blue). Data were fit to the saturation kinetics equation (eq 1) as described in the main text.

of Val27.[2] The tight entrance imposes an energy barrier on the proton conduction because transient N-terminal channel opening is required to admit water or hydronium. The larger opening in the V27A mutant (~5 Å)[15] would greatly facilitate the entrance of water, thereby lowering the energy barrier for proton conduction.

In contrast to V27A, the k_{trans} of S31A is ~62% of WT (Figure 3a, Table S1). Ser31 is the only polar residue between the channel opening at Val27 and His37; it likely plays a role in facilitating pore hydration, which in turn facilitates proton relay to His37. Previous water NOE measurement in the WT and the V27A mutant showed that water molecules are present at around the Ser31 position in the closed state.[2] Therefore replacing Ser31 with alanine may have a negative effect on pore hydration and proton conduction. This interpretation is consistent with the observation that the BM2 channel, a flu B homologue of M2 having three pore-lining serines, has a 2-fold larger conductance than M2 at pH ~6.[16] Although Ser31 increases the hydrophilicity of the pore, it is not absolutely required for conduction; we propose that it simply facilitates the channel hydration, thus decreasing the activation energy for proton relay to His37.

The D44A mutation on the C-terminal side of the His/Trp gating element also decreases the proton flux, with k_{trans} ~55% of that of WT (Figure 3a, Table S1). Asp44 and Arg45 are the only two polar residues in the otherwise hydrophobic portion of the channel.[2,15] Asp44 may assist proton exit by accepting protons or coordinating water molecules. Water molecules were observed around Asp44 and Arg45 in a recent X-ray structure.[4] Replacing Asp44 with alanine may thus increase the activation energy for proton exit.

Based on the above results, we propose a mechanism of proton conduction consisting of three key steps, represented in the reaction scheme below.

$$M2_{InAcc} \underset{k_{-1}}{\overset{k_1}{\rightleftharpoons}} M2_{Acc} \overset{H^+_N}{\underset{k_{-2}}{\overset{k_2}{\rightleftharpoons}}} \left(H^+_N\text{-His}\right)_{M2} \xrightarrow{k_3} H^+_C + M2_{InAcc/Acc} \qquad (2)$$

Step (i) is switching from a H+ inaccessible state ($M2_{InAcc}$) to a H^+ accessible state ($M2_{Acc}$) that allows protons on the N-terminal side ($[H^+_N]$) to reach the pore histidines (k_{-1}/k_1). Step (ii) is proton ($[H^+_N]$) binding to His37 (k_{-2}/k_2). Step (iii) is the irreversible step, in which His37 releases $[H^+_N]$ to proton acceptors on the C-terminal side of the channel gate, thus turning $[H^+_N]$ into $[H^+_C]$ (k_3). We assume step (iii) is irreversible because the conduction is unidirectional from the N to the C terminal end of the channel. Derivation based on the above reaction scheme shows that

$$k_{trans} = k_1k_3/(k_1 + k_3)$$
$$pK_{app} \approx \{-\log(k_{-2}/k_2)\} + \{-\log[(k_1 + k_{-1})/(k_1 + k_3)]\} \qquad (3)$$

The proposed reaction in eq 2 can be described in the context of the channel structure. Initially, the channel is in the closed conformation in which Val27 constriction is too narrow to allow water molecules to freely enter or exit the channel. Channel "breathing" due to thermal energy can transiently enlarge the N-terminal opening, allowing protons to cross the Val27 barrier. This process is represented by the first rate constant k_1. k_1 represents the probability that the channel will admit a proton, which is determined by the rate of channel "breathing", the size of the channel opening, and the hydrophilicity of the channel interior. Therefore, mutating either Val27 or Ser31 should affect the k_1 value. The protons then have to bind to the His37 imidazole. This process is represented by the k_2 rate constant on the kinetic scheme. The histidine protonation triggers conformational rearrangements. First, electrostatic repulsion between protonated imidazoles destabilizes TM helical packing and unlocks the Trp41 indoles that are tightly packed against each other in the closed conformation. The protonated imidazole then forms a cation$-\pi$ interaction with the unlocked Trp41, thus exposing His37 to the high pH environment of the C-terminus. Upon opening of the channel gate, proton acceptors from the C-terminal side (i.e., water molecules) can access His37 and accept protons. This series of steps are represented by the k_3 rate constant on the kinetic scheme. In this step, the polar residue Asp44 and possibly Arg45 increase the presence of water molecules in this region of the channel, thus facilitating hydronium exit.

Acknowledgment. We thank Stephen Harrison, Stephen Blacklow, Donald Coen, James Hogle, Kirill Oxenoid, Adrian Olivares, Jessica Williamson, and Loren Andreas for helpful discussions. This work was supported by grants from the NIH (AI067438 to J.J.C.).

Supporting Information Available: Sample preparation, proton flux assay, proton flux rates, and pH titration. This material is available free of charge via the Internet at http://pubs.acs.org.

References

(1) Pinto, L. H.; Holsinger, L. J.; Lamb, R. A. *Cell* **1992**, *69*, 517–28.
(2) Schnell, J. R.; Chou, J. J. *Nature* **2008**, *451*, 591–5.
(3) Pielak, R. M.; Schnell, J. R.; Chou, J. J. *Proc. Natl. Acad. Sci. U.S.A.* **2009**, *106*, 7379–84.
(4) Acharya, R.; Carnevale, V.; Fiorin, G.; Levine, B. G.; Polishchuk, A. L.; Balannik, V.; Samish, I.; Lamb, R. A.; Pinto, L. H.; DeGrado, W. F.; Klein, M. L. *Proc. Natl. Acad. Sci. U.S.A.* **2010**, *107*, 15075–80.
(5) Wang, C.; Lamb, R. A.; Pinto, L. H. *Biophys. J.* **1995**, *69*, 1363–71.
(6) Tang, Y.; Zaitseva, F.; Lamb, R. A.; Pinto, L. H. *J. Biol. Chem.* **2002**, *277*, 39880–6.
(7) Loria, J. P.; Rance, M.; Palmer, A. G., III. *J. Am. Chem. Soc.* **1999**, *121*, 2331–2332.
(8) Hu, J.; Fu, R.; Nishimura, K.; Zhang, L.; Zhou, H. X.; Busath, D. D.; Vijayvergiya, V.; Cross, T. A. *Proc. Natl. Acad. Sci. U.S.A.* **2006**, *103*, 6865–70.
(9) Chizhmakov, I. V.; Geraghty, F. M.; Ogden, D. C.; Hayhurst, A.; Antoniou, M.; Hay, A. J. *J. Physiol.* **1996**, *494* (Pt 2), 329–36.
(10) Skehel, J. J.; Bayley, P. M.; Brown, E. B.; Martin, S. R.; Waterfield, M. D.; White, J. M.; Wilson, I. A.; Wiley, D. C. *Proc. Natl. Acad. Sci. U.S.A.* **1982**, *79*, 968–72.
(11) Harrison, S. C. *Nat. Struct. Mol. Biol.* **2008**, *15*, 690–8.
(12) Sharma, M.; Yi, M.; Dong, H.; Qin, H.; Peterson, E.; Busath, D. D.; Zhou, H. X.; Cross, T. A. *Science* **2010**, *330*, 509–12.
(13) Hu, F.; Luo, W.; Hong, M. *Science* **2010**, *330*, 505–8.
(14) Okada, A.; Miura, T.; Takeuchi, H. *Biochemistry* **2001**, *40*, 6053–60.
(15) Pielak, R. M.; Chou, J. J. *Biochem. Biophys. Res. Commun.* **2010**, *401*, 58–63.
(16) Wang, J.; Pielak, R. M.; McClintock, M. A.; Chou, J. J. *Nat. Struct. Mol. Biol.* **2009**, *16*, 1267–71.

JA108458U